Catal Lett (2008) 120:19–24
DOI 10.1007/s10562-007-9257-8

Deposition of Gold Particles on Mesoporous Catalyst Supports by Sonochemical Method, and their Catalytic Performance for CO Oxidation

Nina Perkas · Ziyi Zhong · Judit Grinblat · Aharon Gedanken

Published online: 11 September 2007

Abstract Supported gold catalysts on the mesoporous (MSP) metal oxides were prepared by a one-step, ultrasound-assisted reduction method, and characterized by XRD, HRTEM, EDX, BET, and XPS analysis. Their catalytic activities were examined in the oxidation of CO. Compared to the Au/Fe_2O_3(MSP) catalyst, the Au/TiO_2(MSP) and Au/Fe_2O_3-TiO_2(MSP) catalysts exhibited higher catalytic activity in the oxidation of CO at low temperatures. The high catalytic activity of Au/TiO_2(MSP) was attributed to the metallic state of the gold nanoparticles, their small size (2–2.5 nm), and their high dispersion on the catalyst support.

Keywords Sonochemical reduction · Gold · Mesoporous support · CO oxidation

1 Introduction

The low temperature oxidation of CO on highly dispersed gold catalysts is of great interest for many research workers, and more than 120 papers have appeared on this topic during 2006 alone. Since Haruta's publication [1], which demonstrated that small gold particles (less than 10 nm in size) are active in the low temperature CO oxidation, many attempts have been made to achieve a high dispersion of gold nanoparticles on different supports. These methods include classical co-precipitation (CP), deposition—precipitation (DP) [2], incipient wetness impregnation, sol-gel technique, anion and cation adsorption [3], chemical vapor deposition method [4–5], direct anionic exchange [6], and colloid-based method such as one-step synthetic procedure using $NaBH_4$ as the reducing agent and surfactant alkyl trimethyl ammonium bromide as the templating agent [7, 8], and etc. The impregnation method usually provides poor control over the gold particle size. Contrarily, the anionic exchange, cation adsorption, and the colloid-based methods can produce very small gold particles but the gold loading is usually low. So far it seems that CP and DP methods are the most successful in preparing the Au catalysts with high dispersion and high loading of gold particles [3, 9]. However, both of them usually involve a series of procedures, such as long-term thermo stating, washing, drying and calcination, which imposes a big challenge to the ability to maintain the very small size of the gold particles.

Driving from the acoustic cavitation, sonication or ultrasonic irradiation has a variety of physical and chemical effects that can be used to prepare nanosized particles [10, 11]. In addition, as proved in our previous studies [12–14], the sonication can facilitate the deposition of colloidal particles on catalyst support, because during the sonication, very high speed jets and waves with a scale of several hundred meters/second are produced when the bubbles are created and collapse in the liquid solution. These high speedy jets can effectively push the small particles to hit the catalyst supports so as to produce the supported catalysts. In addition, the ultrasonic irradiation method can reduce the metal precursor in situ, thus avoiding the additional heating procedure used in other methods. Herein

N. Perkas · J. Grinblat · A. Gedanken (✉)
Department of Chemistry and Kanbar Laboratory for Nanomaterials, Bar-Ilan University Center for Advanced Materials and Nanotechnology, Bar-Ilan University, Ramat-Gan 52900, Israel
e-mail: gedanken@mail.biu.ac.il

Z. Zhong
Institute of Chemical and Engineering and Sciences, 1 Pesek Road, Jurong Island 627833, Singapore

we report our latest effort to prepare the supported gold catalysts employing the sonochemical method. In this work, the reduction and deposition of the gold particles on the mesoporous catalyst supports are almost conducted simultaneously under the sonication. In order to improve the stability of the gold particles, or reduce their mobility, we make use of mesoporous materials as catalyst supports. These mesoporous supports are TiO_2(MSP), Fe_2O_3(MSP) and Fe_2O_3-TiO_2(MSP), which are also prepared by the sonochemical synthesis [15–17]. All the synthesized mesoporous catalyst supports have a wormhole-like structure and high surface areas. The physicochemical properties of the catalysts are characterized by XRD, HR TEM, EDX, BET and XPS. The catalytic properties are studied in the reaction of CO oxidation.

2 Experimental

All the reagents used were purchased from Aldrich and were of analytical chemical purity. As a gold precursor, a solution of $HAuCl_4$ in HCl was chosen (17 wt% Au content in HCl). The synthesis of Au particles supported on mesoporous supports was carried out by a sonochemical reduction of $HAuCl_4$ under a gas mixture of 95%Ar—5%H_2. For instance, for the preparation of a 1%wt Au/TiO_2(MSP) catalyst, a 0.05 ml solution of $HAuCl_4$ in HCl was dissolved in 100 ml ethanol, followed by the addition of 1 g of TiO_2(MSP) powder, which was prepared by the sonochemical method described elsewhere [15]. The pH value of the slurry was adjusted to 6 with an aqueous solution of ammonia. Before the sonication, the mixture was purged with Ar for 1 h to remove traces of oxygen/air. The purged solution was sonochemically irradiated for 1 h under a gas mixture of 95%Ar—5%H_2 in a 100 ml sonication cell with an immersed high-intensity Ti horn (20 kHz, 45 W/cm^2 at 60% efficiency) on the Sonics and Materials sonofier VCX 600 (Newtown CT, USA). The product was separated by centrifugation, washed three times with a solution of ethanol : aqueous ammonia (1:1), and twice with ethanol for the complete removal of chlorine, then dried overnight in vacuum. The gold catalysts on other mesoporous supports, Au/Fe_2O_3(MSP) and Au/Fe_2O_3-TiO_2(MSP), were prepared similarly using the mesoporous supports synthesized by sonochemical methods [16, 17].

Elemental analysis was carried out by energy dispersed X-ray analysis (EDX) on a JEOL-JSM 840 scanning microscope. The X-ray powder diffraction (XRD) studies were performed on a Bruker D8 diffractometer with Cu-Kα radiation. The catalyst morphology was studied with high resolution transmission electron microscopy. The HRTEM images were obtained on a JEOL-3010 microscope using a 300 kV accelerating voltage. The surface area was measured using a Micromeritics (Gemini 2375) analyzer. The nitrogen adsorption and desorption isotherms were obtained at 77 K after evacuating the sample at 120 °C for 1 h. The surface area was calculated from the linear part of the BET plot. Pore size distribution was estimated using the Barret–Joyner–Halenda (BJH) model with the Halsey equation [18], and the pore volume was measured at the $P/P_o = 0.9947$ signal point. The binding energies of the atoms of interest were determined by X-ray photoelectron spectroscopy (XPS) on a Perkin–Elmer PHI 5000C ESCA spectrophotometer using Mg Kα radiation. The C 1s ($E_b = 285.0$ eV) peak was chosen as a reference line for the calibration of the binding energy.

The measurement of the catalytic oxidation of CO was carried out in a fixed-bed microreactor. Prior to the test, the catalyst was activated under air at 200 °C for 1 h. A reactant gas containing 1% CO in air was passed through the catalyst bed at a GHSV of 15,000 h^{-1}. The outlet gases were analyzed with an on-line GC (Shimadzu).

3 Results and Discussion

3.1 Structure and Morphology of the Catalysts

The gold content in the supports was measured by EDX, and was found to correspond to 1 ± 0.1 wt% in each of the catalysts. This means that almost the entire $HAuCl_4$ precursor used in the reaction was reduced and deposited on the catalyst supports. The chlorine content in the catalysts was also measured by EDX and was found to be less then 0.02 wt% with 10% of standard deviation. This is very important for the catalytic activity of the gold catalysts in CO oxidation [6].

The XRD studies don't show any diffraction peaks on all the three supports, which can be interpreted in the following two ways: (1) the amount of gold, 1%, is below the detection limit of the instrument, or the gold particle size is too small, and (2) the gold is formed in an amorphous state. Information on the morphology and structure of the catalysts was obtained by electron microscopy. In Fig. 1 the HRTEM micrographs are demonstrated. We see that the size of the gold nanoparticles, prepared by the same sonochemical procedure on different supports, is different. On mesoporous TiO_2, the gold nanoparticles are homogeneously distributed and have a diameter of 2–2.5 nm as confirmed by the calculated histogram (Fig. 2).

On the Fe_2O_3·TiO_2(MSP) support, in addition to the small nanoparticles (2–2.5 nm), there are large particles of about 10–20 nm in size (Fig. 1b). The larger gold particles are aggregates of smaller gold nanoparticles, which can be discerned in the HRTEM. On the Fe_2O_3 (MSP) support, we

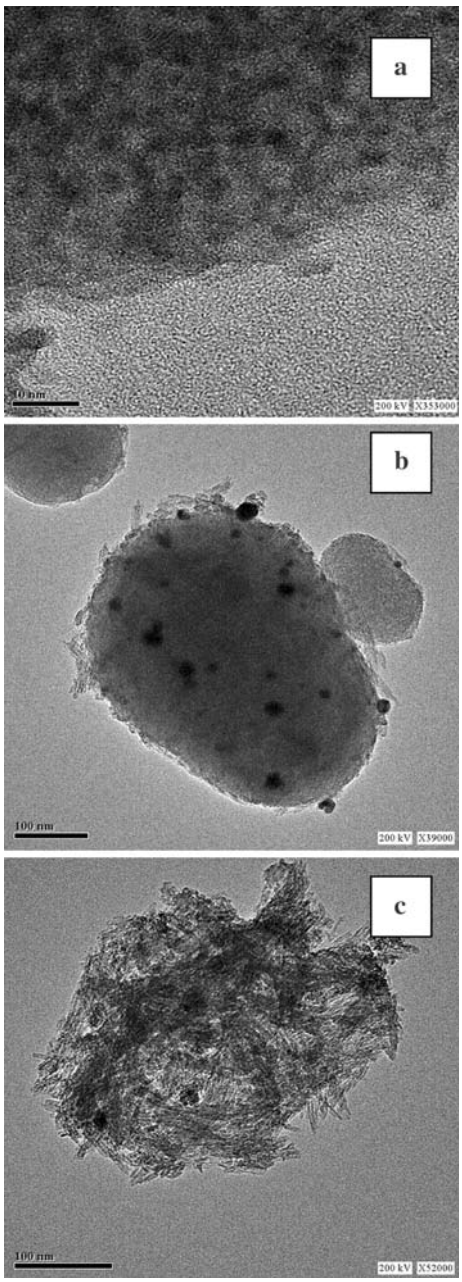

Fig. 1 HR TEM images of the gold supported catalysts: (**a**) Au/TiO_2(MSP)—scale bar 10 nm; (**b**) Au/Fe_2O_3-TiO_2(MSP)—scale bar 100 nm; (**c**) Au/Fe_2O_3(MSP)—scale bar 100 nm

observed the gold particles agglomerated to 20–25 nm in size (Fig. 1c). We did not observe any fringes related to the gold crystal, implying the formation of the amorphous gold as the sonication product. It is well documented that, as a result of the fast cooling rates in sonochemistry, amorphous materials are often obtained as the final products for dispersed [19–21] and supported samples [14, 22, 23].

The HRTEM studies show that the aggregation process depends on the adsorption of gold atoms on the different supports. On the titania support, the gold nanoparticles are

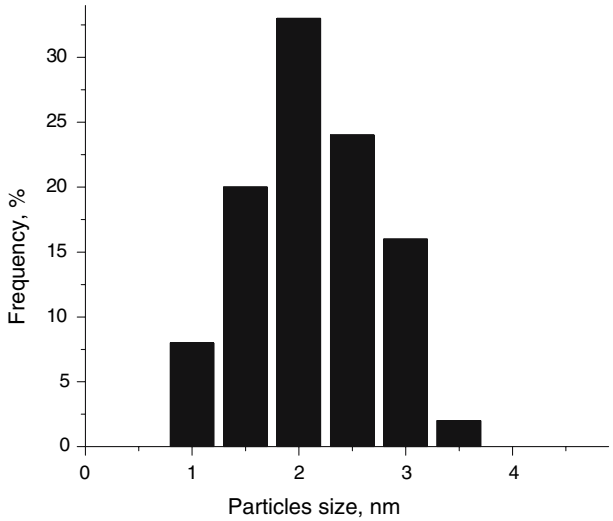

Fig. 2 Histogram of Au/TiO_2(MSP) catalysts

distributed much more homogeneously than on the iron oxide and on the iron oxide-titania composite. The reduction of all the gold ions doesn't occur instantaneously, and during this process every new atom or cluster of gold is thrown at the surface of the support by microjets created after the collapse of the bubbles. The newly formed species are adsorbed either on the support or on the previously deposited gold atoms. Another possibility is that the particles form aggregates before their deposition on the catalyst supports. Obviously, when Fe_2O_3-TiO_2(MSP) or Fe_2O_3(MSP) are used as supports, the adhesion of reduced gold atoms and clusters takes place mostly on the existing centers of gold nucleation.

The BET results presented in Table 1 demonstrate the decrease in the surface area of the supports after the deposition of gold. The pore volume and pore area diminish with the gold deposition. The observed decrease is not very drastic and is attributed to the insertion of a small amount of gold nanoparticles into the pores. This insertion occurs without damaging the pore structure. We have recently reported on similar small changes in the surface structure of mesoporous titania with the insertion/deposition of ruthenium and platinum nanoparticles by the sonochemical method [14, 22].

It should be pointed out that when using TiO_2(MSP) and $Fe_2O_3TiO_2$(MSP) as the catalyst supports, the sizes of the deposited gold nanoparticles are comparable to the average pore diameter of the supports (2–2.5 nm, as measured from HRTEM micrographs). After the deposition of the gold, we observed a decrease of the surface area by 55–60 m^2/g for Au/TiO_2(MSP) and for Au/Fe_2O_3-TiO_2(MSP) catalysts, indicating that the pores of these supports become partially blocked. The decrease in the surface area is higher than that which would be expected by the loading of 1% gold.

Table 1 BET measurements of supported 1 wt% Au catalysts

Catalyst	Surface area (m^2/g)	Pore volume, (ml/g)	Pore size, Å
TiO_2(MSP)	750	0.43	25
Au/TiO_2(MSP)	695	0.41	23
Fe_2O_3-TiO_2(MSP)	650	0.40	22
Au/Fe_2O_3-TiO_2(MSP)	590	0.38	20
Fe_2O_3(MSP)	275	0.31	38
1%Au/ Fe_2O_3(MSP)	225	0.29	36

However, it should be taken into consideration that in TiO_2 (MSP) the pore size is comparable to the gold nanoparticles, and for one pore blocking even one particle of high diameter would be sufficient. Nevertheless, the insertion of the gold particles by the sonochemical method doesn't drastically damage the pores, and the pore size of the TiO_2 (MSP) supports maintains its mesoporous structure intact. The pore size of the Fe_2O_3-TiO_2(MSP) support is smaller than that of TiO_2(MSP), and after the insertion of the gold it is reduced by a larger percentage than in TiO_2(MSP). This argument also explains the localization of gold nanoparticles, mainly on the surface of Fe_2O_3-TiO_2(MSP), as is observed with HR TEM micrographs (Fig. 1b). We did the blank sonochemical experiments in ethanol solution and no changes were observed in the structure and surface area of the mesoporous supports after the sonication in the same ambient conditions (pH, time, gas and temperature) without addition of the gold precursor.

The average diameter of the pores in mesoporous Fe_2O_3 is larger than in the TiO_2(MSP) and Fe_2O_3-TiO_2(MSP) supports (3.8 nm), and the gold nanoparticles can be inserted more easily into the mesopores without their blocking. From the HR TEM image (Fig. 1c), it is also clear that the gold nanoparticles are indeed incorporated into the pores of Fe_2O_3(MSP). We also observed the aggregation of gold to 20–25 nm in the interparticle space of this support. May be there are also very small clusters of gold, unseen by HRTEM, are spread over the support. These clusters are smaller than the optimal size known for the best catalytic activity of gold [24]. Thus in this sample, the gold particles are either too small, or too large. Both of them will lead to a lower catalytic activity.

3.2 XPS Studies

The oxidation state of the gold in the sonochemically prepared catalysts was checked by XPS. The energy value of the Au 4f (7/2) binding region for all the samples was found to be 83.7 eV, lower than that of bulk atoms (84.1 eV) [25]. Probably this can be attributed to the lower coordination number of the surface gold atoms [26]. The same values of binding energy (83.6–83.7 eV) were found for the gold supported on titania by a chemical vapor deposition method [27, 28]. Goodman et al. reported that a significant increase in catalytic activity is caused by the transition of gold particles from a metallic state to a non-metaillic state, which occurs upon reducing the gold particles size to, or below, ca. 5 nm, as well as to the strong metal-support interaction (SMSI) [29–31]. For Au/TiO_2, SMSI is an electron transfer from titania to the supported gold phase, yielding an electron-rich metal layer on highly reduced and defective TiO_x. In our case, the sonochemical synthesis results in the complete reduction of gold, and no positive but negative charged gold clusters was registered by XPS. We attribute the negative charging of the gold particles to an interaction between the gold and the catalyst supports. Probably, it will be beneficial to the improvement of the catalytic performance. It should be pointed out here that on this issue, different opinions exist. For example, Rousset et al. [28] believed that the existence of negatively charged gold clusters is not the main factor for the high activity observed for Au/TiO_2 catalysts, but the metallic gold is the major active phase. In a recent publication, Gates et al. [32] found the positive charging of gold in the Au/Fe_2O_3 catalyst employing a combination of XPS, EXAFS, and other techniques, and proposed that it was cationic gold that acts as the active phase in the conversion of CO.

However, we observed that, for the Au 4f band, the intensity is very different on the three supports. This intensity difference is detected despite the equal 1 wt% concentration of gold in/on the supports (Fig. 3a). The most intense XPS band of gold is detected for the Au/Fe_2O_3-TiO_2(MSP) catalyst, less intense for the Au/TiO_2(MSP), and the weakest for the Au/Fe_2O_3(MSP). We attribute these intensity differences to the different locations of the gold nanoparticles on the catalyst supports. As stated above, in the Au/Fe_2O_3-TiO_2(MSP) catalyst, the major part of the gold is found on the outer surface of the MSP support because these particles can't be inserted into the pores. Thus, the intensity of the gold signal in the Au/Fe_2O_3-TiO_2(MSP) sample is rather high. In the Au/TiO_2(MSP) catalyst, the pores are larger (25 Å), and a larger part of the gold nanoparticles is inserted into the pores. That is why the intensity of the gold band Au 4f (7/2) signal for this sample is weaker. In the Au/Fe_2O_3(MSP) samples, on the one hand, the large aggregates are wrapped by the particles; on the other hand, the very small gold particles are inserted inside the pores (38 Å). As a result, the intensity of the gold signal peak is minimal. These XPS studies are in good agreement with the HRTEM observations, demonstrating the location of gold nanoparticles on the supports.

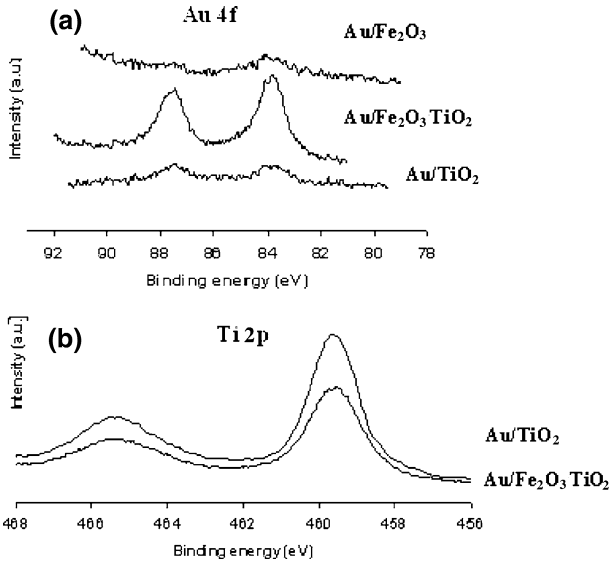

Fig. 3 XPS of the catalysts: (**a**)—Au 4f region; (**b**)—Ti 2p region

For the titania mesoporous support, the binding energy of Ti 2p (459 eV) corresponds to the value of the XPS database reference for TiO_2 [33]. The band intensity of Ti 2p for the Fe_2O_3-TiO_2(MSP) is lower than for the TiO_2(MSP), but no shift is observed in its position (Fig. 3b). The band intensity is lower because there is less Ti in Fe_2O_3-TiO_2 than in TiO_2.

3.3 Catalytic Properties

The gold catalysts prepared by the sonochemical method on different supports demonstrate various activities in CO oxidation. In Fig. 4, the CO conversion is presented as a function of the reaction temperature. It is clear that the nature of the support influences their catalytic performances. A 100% conversion of CO on the Au/TiO_2(MSP) and Au/Fe_2O_3-TiO_2(MSP) catalysts is achieved at 170 and 175 °C, respectively. However, the Au/TiO_2(MSP) catalyst is more active than the Au/Fe_2O_3-TiO_2(MSP), and the half conversion temperature ($T_{50\%}$) on the former (73 °C) is lower by about 70 °C than that of the latter (140 °C). This difference can be rationalized by the existence of the larger aggregates in the Au/Fe_2O_3-TiO_2(MSP) catalyst, as compared with only the small nanoparticles existing in the Au/TiO_2(MSP) catalyst. In contrast, the activity of the Au/Fe_2O_3(MSP) catalyst is the lowest among the three catalysts, and the full conversion of CO is observed only at 225 °C. In this catalyst, the observed gold particle size is either in the range of 20–25 nm (large aggregates), or below 2.5 nm, (the optimal size, ~2.5 nm [30]), hence, its catalytic activity is poorest in comparison with that of the other two supports. It should be noted that all the studied catalysts demonstrate the low temperature conversion of CO, which might have application for the purification of automotive pollution [6].

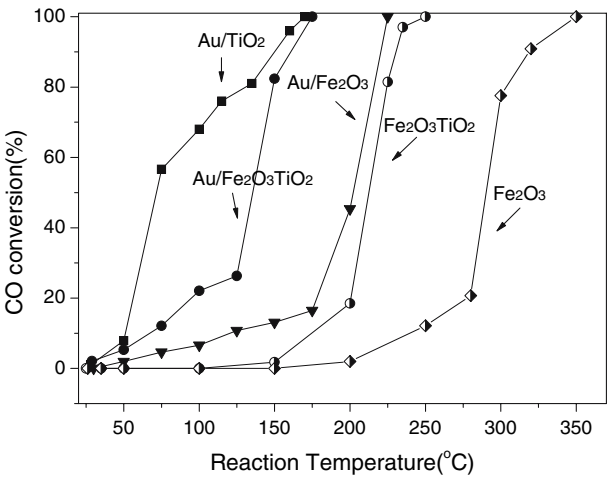

Fig. 4 CO conversion on the gold supported catalysts

The other feature of the three catalysts is their different catalytic performance in the low-temperature range. The light-off temperature for CO oxidation on Au/TiO_2(MSP) is relatively low (50 °C), while for the other two catalysts the light-off temperatures are much higher (125 °C for Au/$Fe_2O_3TiO_2$(MSP) and 175 °C for Au/Fe_2O_3(MSP). The calculated specific activities at 50 °C for the Au/TiO_2(MSP), Au/$Fe_2O_3TiO_2$(MSP) and Au/Fe_2O_3(MSP) are 2.35E-04, 1.58E-04, and 0.60E-04 mol CO/g Au·sec respectively, lower than the best results in literature [5, 34]. Probably there is still a trace of chloride in our catalysts.

To reveal the role of the mesoporous supports in CO oxidation, several control experiment were carried out under the same reaction conditions using bare TiO_2(MSP), Fe_2O_3-TiO_2(MSP), and Fe_2O_3(MSP) oxides as catalysts. The TiO_2(MSP) does not show any catalytic activity in the temperature range of our studies. The activity of Fe_2O_3(MSP) was found to be very low. The 100% conversion of CO with this oxide was achieved at 350 °C (Fig. 4). The mesoporous composite Fe_2O_3-TiO_2(MSP) is more active and demonstrates a full CO conversion at 250 °C. Nevertheless, from the control experiments it follows that the major factor providing CO oxidation at low temperature is the zero-valent gold nanoparticles that are homogeneously distributed on the mesoporous support. This is in agreement with the literature results [27, 35].

After the catalytic reaction we studied the Au/TiO_2(MSP) catalyst by HRTEM and observed some increase in the gold particles size to 3.5–4 nm (Fig. 5). This increase in size can be the reason why the maximal specific activity characteristic for the supported gold nanoclusters of 2–2.5 nm has not be achieved with this catalyst.

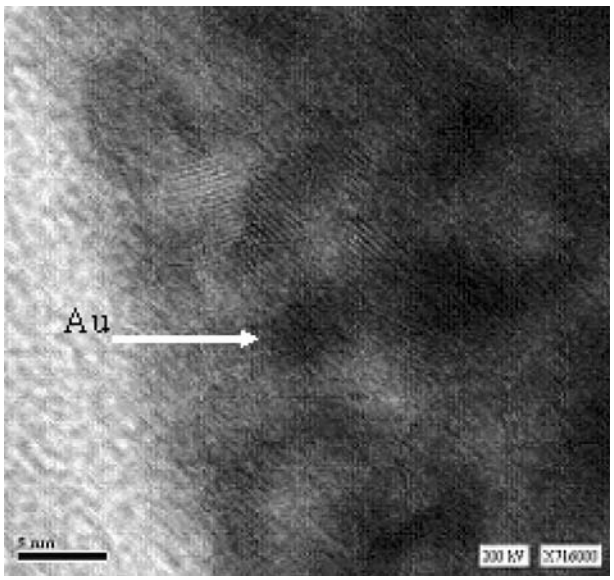

Fig. 5 HR TEM images of the Au/TiO_2(MSP) catalyst—scale bar 5 nm

4 Conclusions

The gold catalysts are prepared by depositing/inserting very small gold particles on/into the mesoporous supports, TiO_2(MSP), Fe_2O_3-TiO_2(MSP), and Fe_2O_3(MSP), employing a one-step ultrasound-assisted reduction method and characterized by XRD, HR TEM, EDX, BET, and XPS analysis. The activity of the catalysts is evaluated in the CO oxidation as a model reaction for the purification of automotive gas pollution. The Au/TiO_2(MSP) demonstrates a complete CO conversion at a low temperature (170 °C). The activity of Au/Fe_2O_3-TiO_2(MSP) is slightly lower, and with the Au/Fe_2O_3(MSP) catalysts the full oxidation of CO was achieved at 225 °C. The difference in the activity of the catalysts is explained by the influence of the geometric factor. The smaller the size of the gold nanoparticles, the higher is the homogeneity of their distribution in the support, and the higher the catalytic activity. The contribution of the support to the CO oxidation is checked by a control reaction, and it is found that the main active component in the catalytic reaction is played by the 2–2.5 nm gold nanoparticles with a zero oxidation state.

References

1. (a) Haruta M, Kobayashi T, Sanmo H, Yamada N (1987) Chem Lett 405; (b) Haruta M, Yamada N, Kobayashi T, Iijima SJ, (1989) Catal 115, 301
2. Park ED, Lee JS (1999) J Catal 186:1
3. Zanella R, Giorgio S, Claude RH, Louis C (2002) J Phys Chem B 106:7634
4. Schimpf S, Lucas M, Mohr C, Rodemerk U, Bruckner A, Radnik U, Hofmeister H, Claus P (2002) Catal Today 72:63
5. Kung HH, Kung MC, Costello CK (2003) J Catal 216:425
6. Ivanova S, Petit C, Pitchon V (2006) Gold Bull 39:3
7. Grunwaldt JD, Kiener C, Wögerbauer C, Baiker A (1999) J Catal 181:223
8. Liu J-H, Chi Y-C, Lin H-P, Mou C-Y, Wan B-Z (2004) Catal Today 93–95:141
9. Landon P, Ferguson J, Solsona BE, Garcia T, Carley AF, Herzing AA, Kiely CJ, Golunski SE, Hutchings GJ (2005) Chem Comm 3383
10. Suslick KS, Hyeon TW, Fang MW (1996) Chem Mater 8:2172
11. Gedanken A (2004) Ultrason Sonochem 11:47
12. Zhong Z, Prozorov T, Felner I, Gedanken A (1999) J Phys Chem B 103:947
13. Gedanken A, Tang X, Wang Y, Perkas N, Koltypin Y, Landau MV, Vradman L, Herskowitz M (2001) Chem Eur J 7:4547
14. Perkas N, Zhong Z, Chen L, Besson M, Gedanken A (2005) Catal Lett 103:9
15. Wang YQ, Tang XH, Gedanken A (2000) Adv Mater 12:1137
16. Srivastava DN, Perkas N, Gedanken A, Felner I (2002) J Phys Chem B 106:1878
17. Perkas N, Plachik O, Brukental I, Nowik I, Gofer Y, Koltypin Y, Gedanken A (2003) J Phys Chem B 107:8772
18. Gregg SJ, Sing KS (1982) Adsorption surface area and porosity. Academic Press, London p 37
19. Zhong Z, Chen F, Subramanian AS, Lin J, Highfield J, Gedanken A (2006) J Mater Chem 16:489
20. Dhas NA, Cohen H, Gedanken A (1997) J Phys Chem B 101:6834
21. Salkar RA, Jeevanandam P, Aruna ST, Gedanken A (1999) J Mater Chem 9:1333
22. Perkas N, Pham Minh D, Gallezot P, Gedanken A, Besson M (2005) Appl Catal B 59:121
23. Pol VG, Wildermuth G, Felsche J, Gedanken A, Calderon-Moreno JJ (2005) Nanosize and Nanotech 5:975
24. Chen MS, Goodman DW (2006) Catal Today 111:22
25. Anthony MT, Seah MP (1984) Surf Interface Anal 6:95
26. Citrin PH, Wertheim GK, Bayer Y (1978) Phys Rev Let 41:1425
27. Radnik J, Mohr K, Claus P (2003) Phys Chem Chem Phys 5:172
28. Arrii S, Morfin F, Renouprez AJ, Rousset JL (2004) J Am Chem Soc 126:1199
29. Valden M, Lai X, Goodman DW (1998) Science 281:1647
30. Chen MS, Goodman DW (2004) Science 306:252
31. Goodman DW (2005) Catal Lett 99:1
32. Hutching GH, Hall MS, Carley AF, Landon P, Solsona BE, Kiely CJ, Herzing A, Makkee M, Moulijn JA, Overweg A, Fierro-Gonzalez JC, Guzman J, Gates BC (2006) J Catal 24:71
33. Burke AR, Brown CR, Bowling WC, Glaub JE, Karsch D, Love CM, Whitakev RB, Moddeman WE (1988) Surf Interface Anal 11:353
34. Khoudiakov M, Gupta MC, Deevi S (2005) Appl Catal 291:151
35. Zwijnenburg A, Goossens A, Sloof WG, Craje WJ, Van der Kraan AM, Jos de Jongh L, Makkee M, Moulijn A (2002) J Phys Chem B 106:9853